Korean J. of Chem. Eng., 7(1) (1990) 47-52

MASS TRANSFER IN TWO-AND THREE-PHASE FLUIDIZED BEDS

Ihl-Yong KIM and Sang Done KIM*

Department of Chemical Engineering, Korea Advanced Institute of Science and Technology, Seoul 130-650, Korea

(Received 14 June 1989 • accepted 24 July 1989)

Abstract—The effects of liquid (0.03-0.12 m/s) and gas (0.04-0.20 m/s) velocities, and particle size (0-8.0 mm) on the volumetric mass transfer coefficients at the grid zone have been determined in a 0.152 m-I.D. × 1.8 m high Plexiglas column.

The volumetric mass transfer coefficient in the grid zone increases with increasing gas velocity and particle size. However, the coefficient exhibits a maximum value at an optimum bed porosity condition.

The volumetric mass transfer coefficients in terms of the Sherwood number in three-phase fluidized beds have been correlated with the Schmidt number and particle Reynolds number which is related to the energy dissipation rate in the beds based on the local isotropic turbulence theory. Also, the coefficient has been correlated with the experimental variables.

INTRODUCTION

Recently, three-phase fluidized bed reactors are widely used in the field of chemical and biochemical processes. Therefore, the mass transfer characteristics in two- and three-phase fluidized beds have to be studied to provide prerequisite knowledge for designing three-phase fluidized bed reactors.

In three-phase fluidized beds, the gas-liquid mass transfer can be affected by the presence of solid particles and it was found to be liquid-phase controlled in many cases [1,2]. Therefore, the liquid-side mass transfer coefficient is needed for the design of three-phase reactors. However, most of previous studies have been confined within low gas and liquid velocities, and the mass transfer characteristics of grid zone of bubble columns and three-phase fluidized beds are very limited.

Initially, the mass transfer coefficient has been measured by Massimilar et al. [3]. It has been found that the gas-liquid mass transfer was the major rate determining step of the overall process in three-phase fluidized beds. Ostergaard et al. [4,5] reported that the volumetric mass transfer coefficient (k_La) in the beds of 5 mm glass beads is greater than that in the beds of 1 mm glass beads since the larger particles break the bubbles in the bed. Also, k_La decreases with column height in bubble columns and three-phase fluidized beds of 1 mm glass beads where bubble coalescence takes place and k_La exhibits a maximum value with the variation of column height in the bed of 6 mm glass beads. Recently, Chang et al. [2] determined the effect of ionic strength of liquid phase on k_La and gas-liquid interfacial area, a, in three-phase fluidized beds.

The two-zone model has been proposed by Alvarez-Cuenca et al. [6] for analyzing the mass transfer coefficient in bubble columns and three-phase fluidized beds, and reported that the most of mass transfer takes place at the grid zone near the distributor due to the jet turbulence in comparison to that in the bulk zone.

Therefore, in this study, the effects of liquid (0.03-0.12 m/s) and gas (0.04-0.20 m/s) velocities and particle size (0.0-8.0 mm) on k_La at the grid zone have been determined in bubble columns and three-phase fluidized beds.

EXPERIMENTAL

Experiments were carried out in a relatively large Plexiglas column 0.152 m-I.D. × 1.8 m-high as shown in Fig. 1. Solid particles were supported on a perforated plate containing 156 evenly-spaced holes of 3.0 mm diameter which served as the liquid phase distributor. The distributor was situated between the main

*To whom all correspondence should be addressed.

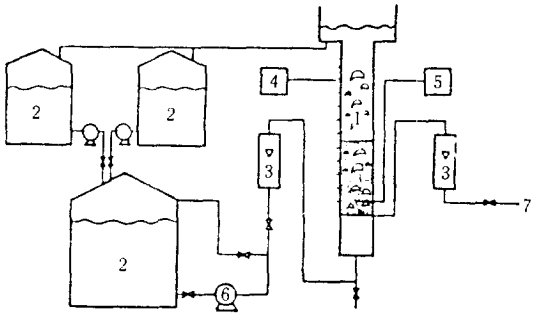

Fig. 1. Experimental apparatus.

1. Main column
2. Liquid reservoir
3. Flowmeter
4. Pressure tap
5. Oxygen meter
6. Pump
7. Compressed air

column section and a 0.3 m high stainless steel distributor box into which the liquid phase was introduced through a 25.4 mm pipe from the reservoir. The liquid flow rate was measured with a flowmeter and regulated by means of globe valves on the feed and bypass lines.

Oil-free compressor air was fed to the column through four evenly spaced 6.35 mm I.D. perforated feed pipes which contained 26 holes of 1.0 mm diameter drilled horizontally through the grid. The pipes were evenly spaced across the distributor plate. This arrangement allows the gas and liquid were introduced into the bed separately. Ten pressure taps were mounted flush with the wall of the column at 0.1 m height intervals.

Throughout this study, tap water was used as the liquid phase, air as the gas phase and either 1.7, 3.0, 6.0 or 8.0 mm glass beads, each with a density of 2500 kg/m^3 as the solid phase. Superficial velocities of liquid and gas phases ranged from 0.03 to 0.12 m/s and from 0.04 to 0.20 m/s, respectively.

The gas and liquid were introduced into the bed of solids at the desired superficial velocities. When the column operation was reached steady state, the pressure profile up to the entire height of the column was measured by using liquid manometers.

The expanded bed height was taken as the point at which a change in the slope of the plot was observed [2,7]. The expanded bed height so obtained agreed well with those of visual observations. The liquid and gas phase holdups were determined from the knowledge of pressure drop, expanded bed height, and fluid and solid properties [7].

Liquid sample was withdrawn at 110 mm from the distributor. The sampling bottle as a gas-liquid separator consists of an upward facing orifice, an incoming liquid flow inlet port and an outlet nozzle. The dissolved oxygen concentration in water in the column was measured by using a dissolved oxygen meter (Beckman model 0260). To avoid liquid film resistance for diffusion of oxygen towards the electrode, the sampled liquid was stirred vigorously by using a magnetic stirrer. To maintain a constant solubility of O_2 in the liquid, the liquid temperature was maintained at 23 ± 2°C. The Na_2SO_3 solution was used to deaerate the oxygen-saturated water. The oxygen dissolved water in the column was collected in a reservoir tank in which 20% Na_2SO_3 solution was added for deaeration. The deaerated liquid sent to the main liquid tanks and it was introduced into the main column.

Determination of volumetric mass transfer coefficients

The volumetric mass transfer coefficients of the grid zone are calculated by the plug flow model [8]. The material balance and the boundary conditions of the grid zone can be given as:

$$dC/dy = \alpha (C^* - C) \qquad 0 \le y \le b \tag{1}$$

$$C = C_o = C(0) \qquad y = 0 \tag{2}$$

The dissolved oxygen concentration at the grid zone from the above equations become:

$$C = C^* - (C^* - C_o)\exp(-\alpha y) \tag{3}$$

From Eq. (3), the parameter $\alpha = (k_L a)_{TG}/U_l$ was determined from the experimental data where the $(k_L a)_{TG}$ represents the volumetric mass transfer coefficient in the grid zone.

RESULTS AND DISCUSSION

1. Liquid-gas system

The height of grid zone has been found to be varied from 0.07 to 0.11 m from the grid depending on the velocities of fluids. At the moment of bubble formation, the gas or bubble surface continuously exposed to liquid phase, and as a result the gas actively circulating inside the bubbles and the gas/liquid mass transfer take place due to the interaction between the liquid and gas jets close to the distributor [1].

The effect of gas velocity on $(k_L a)_{TG}$ in bubble columns is shown in Fig. 2. As can be seen in Fig. 2, $(k_L a)_{TG}$ increases with an increase in gas velocity. In batch bubble columns [9-11] and in a gas-liquid cocurrent flow systems [12], the dependency of gas velocity on the volumetric mass transfer coefficient is found to be very similar to that observed in the present systems. Also, the effect of liquid velocity on the volumetric mass transfer coefficient is found to be very

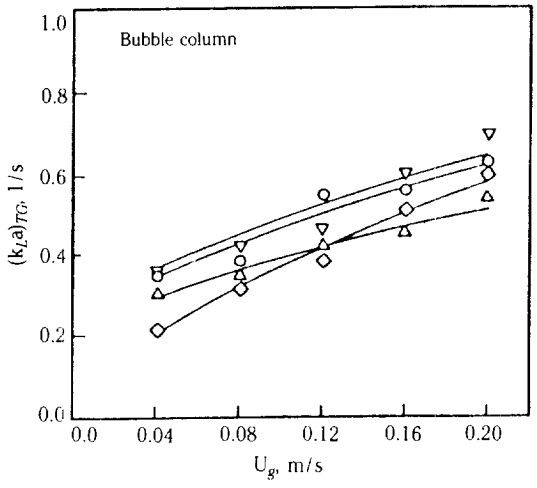

Fig. 2. Effect of gas velocity on $(k_La)_{TG}$ in bubble columns.
U_l(m/s): △; 0.04, ○; 0.06, ▽; 0.10, ◇; 0.12

small.

The obtained volumetric mass transfer coefficients in the present gas-liquid cocurrent flow system have been correlated as:

$$(k_La)_{TG}=0.155U_g^{0.415}U_l^{0.073} \quad (4)$$

with a multiple correlation coefficient of 0.85 with the standard deviation of 0.197. This correlation covers the range of variables $0.04\leq U_g\leq 0.20$ m/s and $0.04\leq U_l\leq 0.12$ m/s.

The bubble diameter in cocurrent gas and liquid flow systems has been represented by Jin et al. [13] as:

$$d_b=0.836U_g^{0.471}U_l^{-0.029} \quad (5)$$

If the bubble size in the grid zone is assumed to have a spherical shape with an uniform size, the following relation can be applied.

$$d_b=6\epsilon_g/a \quad (6)$$

Combining Eqs. (4), (5) and (6) with the eddy cell model [14], the mass transfer coefficient in terms of the Sherwood number in the grid zone can be correlated as:

$$Sh_b=12.17Sc^{0.50}Re_b^{0.24} \quad (7)$$

with a correlation coefficient of 0.94 with the standard deviation of 0.18. Those exponents in Eq. (7) are well accord to the eddy cell model ($Sc^{1/2}Re^{1/4}$).

2. Three-phase fluidized beds

The effect of gas velocity on the volumetric mass transfer coefficient of the grid zone $(k_La)_{TG}$ in three-phase fluidized beds is shown in Fig. 3. As can be seen

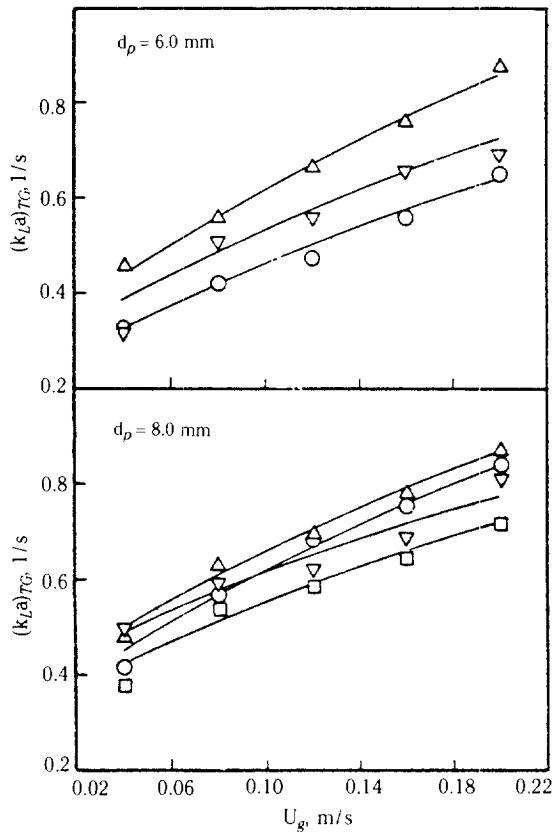

Fig. 3. Effect of gas velocity on $(k_La)_{TG}$ in three-phase fluidized beds.
d_p = 6.0 mm: U_l (m/s): ○; 0.07, △; 0.08, ▽; 0.12,
d_p = 8.0 mm: U_l (m/s): ○; 0.08, △; 0.09, ▽; 0.10, □; 0.12

in Fig. 3, $(k_La)_{TG}$ increases with increasing gas velocity [2,15].

The energy dissipation rate of the liquid phase based on the local isotropic turbulence theory [2,16-18] can be calculated from the knowledge of individual phase holdups, fluid properties and its velocities as

$$E_D=\frac{[(U_l+U_g)(\epsilon_g\rho_g+\epsilon_l\rho_l+\epsilon_s\rho_s)-U_l\rho_l]g}{\epsilon_l\rho_l+\epsilon_s\rho_s} \quad (8)$$

Since the mass transfer coefficient, k_L, is mainly governed by the small-scale eddies in the turbulent field [14,19], the coefficient increases due to the increase of energy dissipation rate with an increase in gas velocity (Eq. 8). Consequently, the increased volumetric mass transfer coefficient may come from the increase of the gas-liquid interfacial area and the mass transfer coefficient with an increase in gas velocity.

The effect of liquid velocity on the volumetric mass

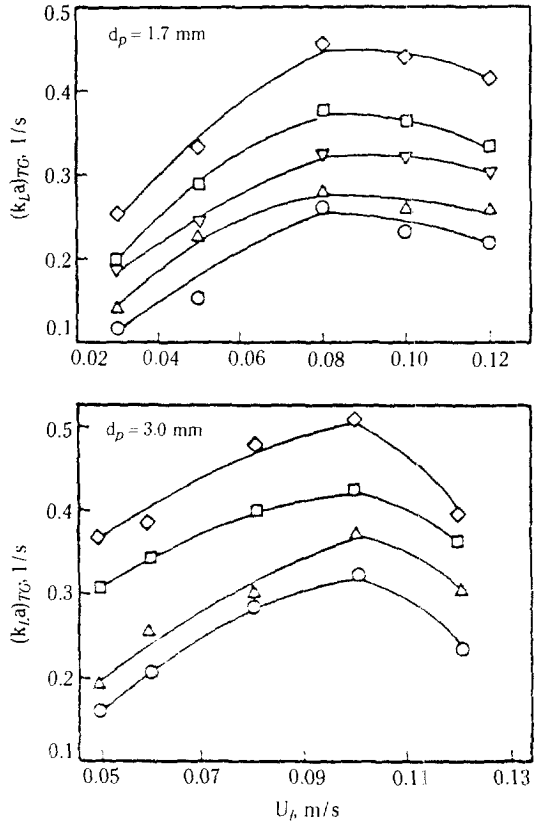

Fig. 4. Effect of liquid velocity on $(k_La)_{TG}$ in three-phase fluidized beds.
U_g (m/s): ○; 0.04, △; 0.08, ▽; 0.12, □; 0.16, ◇; 0.20

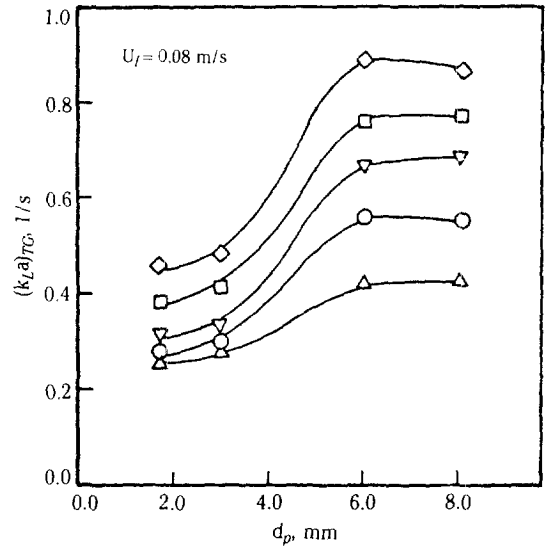

Fig. 5. Effect of particle size on $(k_La)_{TG}$ in three-phase fluidized beds.
U_g (m/s): △; 0.04, ○; 0.08, ▽; 0.12, □; 0.16, ◇; 0.20

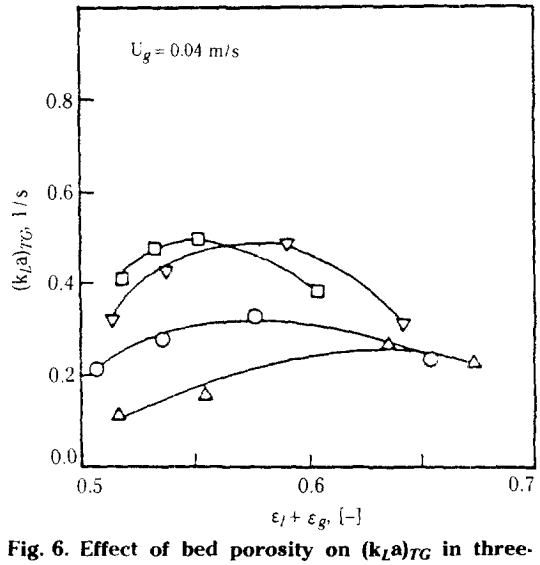

Fig. 6. Effect of bed porosity on $(k_La)_{TG}$ in three-phase fluidized beds.
d_p(mm): △; 1.7, ○; 3.0, ▽; 6.0, □; 8.0

transfer coefficient in three-phase fluidized beds of 1.7, 3.0, 6.0, 8.0 mm glass beads can be seen in Fig. 4. As can be seen, the volumetric mass transfer coefficient increases with an increase in liquid velocity in three-phase fluidized beds. In three-phase fluidized beds, the volumetric mass transfer coefficient increases due to the increases of gas-liquid interfacial area and of the energy dissipation rate (Eq. 8) with an increase in liquid velocity, since the bubble size decreases with an increase in liquid velocity [13,20].

The effect of particle size on the volumetric mass transfer coefficient can be seen in Fig. 5. As one can see in Fig. 5, the volumetric mass transfer coefficient increases with an increase in particle size.

Two distinct types of three-phase fluidized beds, namely bubble-coalescing and bubble-disintegrating beds, have been known to exist [7]. It has been found in previous studies [7,13,20] that the bubble sizes in bubble coalescing beds (d_p = 1.0, 1.7, 2.3 mm) are larger than those in the bubble disintegrating beds (d_p = 3.0, 6.0, 8.0 mm) and the gas phase holdups in bubble disintegrating beds (d_p = 3.0, 6.0, 8.0 mm) and the gas phase holdups in bubble coalescing beds are smaller than those in the bubble disintegrating beds. Therefore, $(k_La)_{TG}$ increases with an increase in particle size since the gas-liquid interfacial area increases with increasing gas phase holdup and with decreasing bub-

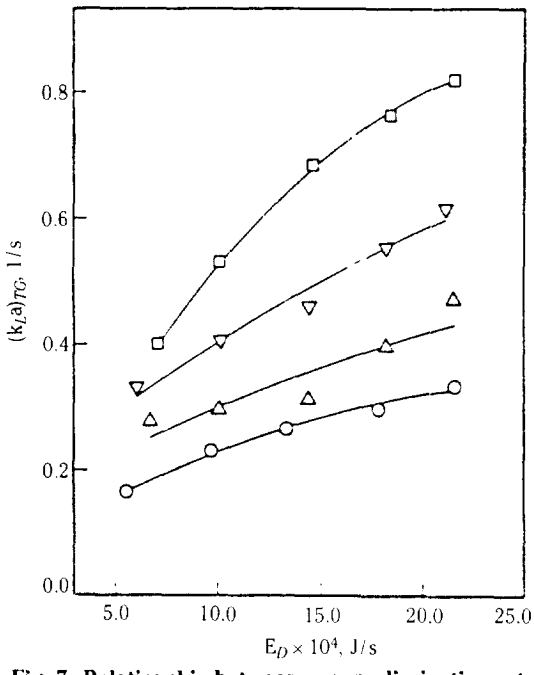

Fig. 7. Relationship between energy dissipation rate and $(k_La)_{TG}$ in three-phase fluidized beds.
d_p(mm): ○; 1.7, △; 3.0, ▽; 6.0, □; 8.0

ble size. The increase of volumetric mass transfer coefficients with particle size has been reported by previous investigators [2,15].

The effect of bed porosity on $(k_La)_{TG}$ in three-phase fluidized beds is shown in Fig. 6. As can be seen, $(k_La)_{TG}$ exhibited a maximum value at bed porosity range of 0.55-0.65 [2]. Same trend has been observed in the study of heat transfer in three-phase fluidized beds [21-25].

The effect of energy dissipation rate on the volumetric mass transfer coefficient in three phase fluidized beds is shown in Fig. 7. As can be seen, the volumetric mass transfer coefficient increases with an increase in energy dissipation rate. Also, the volumetric mass transfer coefficient increases with an increase in particle size at a similar energy dissipation rate since the bubble size decreases and gas phase holdup increases with increasing particle size [7,13,20].

CORRELATIONS

The volumetric mass transfer coefficient, $(k_La)_{TG}$, in three-phase fluidized beds (d_p = 1.7, 3.0, 6.0, 8.0 mm) have been correlated with the Schmidt number and particle Reynolds number which is related to the energy dissipation rate in the bed based on the local isotropic turbulence theory.

$$Sh_p = \frac{(k_La)_{TG} d_p^2}{D} = 0.207 Sc^{-0.5} Re_p^{0.64} \quad (9)$$

with a multiple correlation coefficient of 0.99.

In order to determine the effects of each experimental variables on $(k_La)_{TG}$, the present experimental data have been correlated with the experimental variables as:

$$(k_La)_{TG} = 0.203 U_g^{0.388} (0.3 + 36.4 U_l^{0.94} - 2.02 \times 10^2 U_l^{2.04})^{1.41} d_p^{0.471} \quad (10)$$

with a multiple correlation coefficient of 0.95. This correlation covers the range of variables $0.04 \leq U_g \leq 0.20$ m/s, $0.03 \leq U_l \leq 0.12$ m/s and $1.7 \leq d_p \leq 8.0$ mm.

CONCLUSIONS

In bubble columns and three-phase fluidized beds, the volumetric mass transfer coefficient, $(k_La)_{TG}$, in the grid zone increases with increasing gas velocity. However, the rate of increase in $(k_La)_{TG}$ decreases with increasing gas velocity. The $(k_La)_{TG}$ exhibits a maximum value with a liquid velocity or bed porosity. The $(k_La)_{TG}$ increases with increasing particle size in three-phase fluidized beds.

The mass transfer coefficient in terms of the Sherwood number is correlated in terms of the bubble Reynolds number in bubble columns. In three-phase fluidized beds, the volumetric mass transfer coefficients in terms of the Sherwood number were correlated with the Schmidt and particle Reynolds numbers which is related to the energy dissipation rate in the beds based on the isotropic turbulence theory.

NOMENCLATURE

a	:	gas/liquid interfacial area, [m^{-1}]
b	:	sampling position from the distributor, [m]
C	:	concentration of the liquid, [mg/ℓ]
C^*	:	equilibrium concentration of the liquid, [mg/ℓ]
C_0	:	inlet concentration of the liquid, [mg/ℓ]
D	:	diffusivity, [m^2/s]
d_b	:	bubble diameter, [m]
E_D	:	energy dissipation rate based on the fluidized bed, [m^3/s]
g	:	gravitational acceleration, [m/s^2]
k_L	:	liquid phase mass transfer coefficient, [m/s]
k_La	:	volumetric mass transfer coefficient, [1/s]
Re_b	:	Reynolds number of liquid flow, $E_D d_b^4/\nu^3$
Re_p	:	particle Reynolds number, $E_D d_p^4/\nu^3$
Sc	:	Schmidt number, ν/D
Sh_b	:	bubble Sherwood number, $k_L d_b$/D

Sh_p : particle Sherwood number, $k_L a d_p^2/D$
U : superficial velocity, [m/s]
U_{mf} : minimum fluidizing velocity, [m/s]
y : distance, [m]

Greek Letters

α : constant
ν : kinematic viscosity, [m^2/s]
ϵ : phase holdup, [-]
ρ : density, [kg/m^3]

Subscripts

g : gas phase
l : liquid phase
s : solid phase
TG : grid zone

REFERENCES

1. Alvarez-Cuenca, M. and Nerenberg, M.A.: *Can. J. Chem. Eng.*, **59,** 739 (1981).
2. Chang, S.K., Kang, Y. and Kim, S.D.: *J. Chem. Eng. Japan*, **19,** 524 (1986).
3. Massimilla, L., Majuri, N. and Squillance, E.: *Brit. Chem. Eng.*, **6,** 232 (1959).
4. Ostergaard, K. and Suchzebraski, W.: Chem. Reaction Eng. Progr., 4th European Symp. Sept., (1969).
5. Ostergaard, K. and Fosbol, P.: *Chem. Eng. J.*, **3,** 105 (1972).
6. Alvarez-Cuenca, M., Baker, C.G.J. and Nerenberg, M.A.: *Can. J. Chem. Eng.*, **61,** 58 (1984).
7. Kim, S.D., Baker, C.G.J. and Bergougnou, M.A.: *Can. J. Chem. Eng.*, **53,** 134 (1975).
8. Alvarez-Cuenca, M. and Nerenberg, M.A.: *AIChE J.*, **27,** 66 (1982).
9. Akita, K. and Yoshida, F.: *Ind. Eng. Chem. Process Des. Dev.*, **12,** 76 (1973).
10. Hikita, H., Asai, S., Tanigawa, K., Segawa, K. and Kitao, M.: *Chem. Eng. J.*, **22,** 61 (1981).
11. Shah, Y.T., Keilor, B.G., Godbole, S.P. and Deckwer, W.D.: *AIChE J.*, **28,** 353 (1982).
12. Deckwer, W.D., Nguyen-Tien, K., Kelkar, B.G. and Shah, Y.T.: *AIChE J.*, **29,** 915 (1983).
13. Jin, G.T., Kim, S.D. and Choi, I.S.: Proc. World Congress III of Chem. Eng. Tokyo, 2, 492 (1986).
14. Lamont, J.C. and Scott, D.S.: *AIChE J.*, **16,** 513 (1970).
15. Nguyen-Tien, K., Patwari, A.N., Shumpe. A. and Deckwer, W.D.: *AIChE J.*, **31,** 194 (1985).
16. Sanger, P. and Deckwer, W.D.: *Chem. Eng. J.*, **22,** 179 (1981).
17. Suh, I.S., Jin, G.T. and Kim, S.D.: *Multiphase Flow*, **11,** 255 (1985).
18. Magiliotou, M., Chen, Y.M. and Fan, L.S.: *AIChE J.*, **34,** 1043 (1988).
19. Calderbank, P.H. and Mooyoung, M.B.: *Chem. Eng. Sci.*, **16,** 39 (1961).
20. Kim, J.O. and Kim, S.D.: *Particulate Sci. and Technol.*, **5,** 309 (1987).
21. Baker, C.G.J., Armstrong, E.R. and Bergougnou, M.A.: *Powder Technol.*, **21,** 195 (1978).
22. Chiu, T.M. and Nerenberg, M.A.: Proc. of 6th Int. Ferment. Symp. Series, London, Canada, 477, Pergamon Press, New York (1980).
23. Kang, Y., Suh, I.S. and Kim, S.D.: *Chem. Eng. Commun.*, **34,** 1 (1985).
24. Kim, S.D., Kang, Y. and Kwon, H.K.: *AIChE J.*, **16,** 513 (1986).
25. Kim, S.D., Lee, Y.J. and Kim, J.O.: *Exp. Thermal and Fluid Sci.*, **1,** 237 (1988).